

A self-microemulsion enhances oral absorption of Docetaxel by inhibiting P-glycoprotein and CYP metabolism

Le Tong

Jinzhou Medical University

ZeYang Zhou

GuangXi University of Chinese Medicine

Gang Wang

GuangXi University of Chinese Medicine

Chao Wu (✉ wuchao@jzmu.edu.cn)

Jinzhou Medical University

Research Article

Keywords: SMEs, Docetaxle, Curcumin, P-gp, CYP 450, Oral bioavailability

Posted Date: September 29th, 2022

DOI: <https://doi.org/10.21203/rs.3.rs-2041625/v1>

License:  This work is licensed under a Creative Commons Attribution 4.0 International License.

[Read Full License](#)

Abstract

Oral absorption of docetaxel was limited by drug efflux pump p-glycoprotein (P-gp) and cytochrome P450 enzyme (CYP 450). Therefore, co-loading agent that inhibits P-gp and CYP 450 in self-nanoemulsifying drug delivery system (SMEs) is considered as a promising strategy for oral delivery of docetaxel. In this study, curcumin was selected as an inhibitor of P-gp and CYP 450, and it was coencapsuled in SMEs to improve the oral bioavailability of docetaxel. SMEs quickly dispersed in water within 20 seconds, and the droplet size was 32.23 ± 2.21 nm. The release rate of curcumin from DC-SMEs was higher than that of docetaxel in vitro. Compared with free docetaxel, SMEs significantly increased the permeability of docetaxel by 4.6 times. And competitive experiments showed that the increased permeability was the result of inhibition of p-gp. The half-life and oral bioavailability of DC-SMEs increased about 1.7 times and 1.6 times than docetaxel SMEs, which indicated that its good pharmacokinetic behavior was related to the restriction of hepatic first-pass metabolism. In conclusion, DC-SMEs was an ideal platform to facilitate oral delivery of docetaxel through inhibited P-gp and CYP 450.

Introduction

Oral administration has become the first choice in clinics due to its safety and convenience, while chemotherapy drugs are still mainly through intravenous route. The main limitations of oral chemotherapy are poor solubility and permeability, especially for BCS IV antitumor drugs [1]. Therefore, how to improve poor oral bioavailability is the key to the development of oral chemotherapeutic agents.

Docetaxel as the first line antitumor agent was currently used for prostate cancer, non-small cell lung cancer (NSCLC) [2–3]. The recommended dose schedule was intravenously administered docetaxel every 3 weeks, which was restricted by myelosuppression in clinic. Although weekly docetaxel was less toxic [4], it was rarely used in practice because of its inconvenience to patients. To address these challenges, docetaxel oral solid dispersion formulations have been developed and evaluated in clinical trials, including ModraDoc001 capsule, ModraDoc006 tablet [5–6]. Unfortunately, limited oral bioavailability caused therapeutic failures. In addition, various nano-formulations including self-nanoemulsifying drug delivery system (SMEs) [7], PLGA nanoparticles [8], solid lipid nanoparticles [9] and milk [10] have been adopted for oral delivery of docetaxel. Among these nanosystems, SMEs was considered as an ideal oral drug delivery strategy because of its high solubilization potential and thermodynamic stability [11]. SMEs was a lipid-based oral drug delivery system, which was composed of oil, emulsifier and co-emulsifier. When exposed to an aqueous environment of gastrointestinal tract (GI), a water-containing (O/W) type microemulsion will be automatically formed. Thus, the drug molecules within SMEs not only enhanced solubility and membrane permeability, but also the stability against GI environment. SMEs has been applied to a series of drugs, including docetaxel and nifedipine [7, 12]. However, oral absorption of SMEs loaded docetaxel was still hampered by P-gp and CYP 450 [5]. To address these issues, co-administration of the CYP450 inhibitor ritonavir was a feasible scheme. However, different pharmacokinetic behaviors and dose limited toxicity (diarrhea) in phase I clinical trial affected the development of oral docetaxel [13]. Cui et al. reported a novel SMEs for the oral co-delivery of docetaxel and cyclosporine A (CsA), which

strongly enhanced the oral bioavailability of docetaxel [14]. Although CsA has great potential in improving the oral absorption of docetaxel, its use in clinical application still faced great challenge due to its acute nephrotoxicity, severe hypertension and neurotoxicity [15–16].

Curcumin, a natural polyphenol, exhibits several pharmacological effects including anti-oxidant and anti-inflammatory [17]. Several studies have demonstrated that curcumin was a potent inhibitor of P-gp and has been frequently used for reversing P-gp mediated efflux [18]. Some evidence suggested that the combination of curcumin can effectively enhance the treatment of docetaxel [19–20]. Curcumin was also reported as an effective inhibitor of CYP450 and the IC_{50} of CYP3A4 was $11.93 \pm 3.49 \mu\text{M}$ [21]. Thus, the down-regulation of intestinal CYP3A in vivo could significantly improve the oral bioavailability of drugs with strong first pass metabolism. Curcumin was generally considered to be a safe compound for human beings, even if the oral doses of 8 g/day for 3 months [22]. However, instability, strong hydrophobicity and rapid metabolism in the GI tract resulted in a low oral bioavailability of curcumin. Thus, we hypothesized that encapsulation of docetaxel and curcumin into SMEs could improve the oral bioavailability and therapeutic effect.

Herein, we reported a unique co-loaded SMEs for efficient oral delivery of docetaxel and curcumin. The prepared SMEs was optimized by simplex lattice method analysis and characterized by the droplet size, zeta potential, morphology, stability and in vitro drug release. The permeability of SMEs was studied by using Caco-2 cell monolayer. Finally, pharmacokinetics study was conducted in rats to evaluate the oral bioavailability of co-loaded SMEs. In this study, we demonstrated that co-loaded SMEs significantly increased the oral bioavailability of docetaxel by inhibiting of P-gp and CYP 450 enzyme.

Materials And Methods

Materials

Cremophor® EL40 was purchased from Shanghai Macklin Biochemical Co., Ltd. Tween 80 was purchased from Tian Jin Fu Yu Chemical Co., Ltd. Docetaxel (purity 98%), curcumin (purity 98%), 1,3-propanediol, PEG400, diethylene glycol monoethyl ether (DGME) and tween 20 were purchased from Shanghai Aladdin Bio-Chem Technology Co.,Ltd. Isopropyl myristate, ethyl oleate and medium chain triglycerides (MCT) were purchased from Shanghai yuanye Bio-Technology Co., Ltd.; Caco-2 cells were obtained from ATCC.

Solubility Of Docetaxel (D) and Curcumin (C)

The solubilities of docetaxel and curcumin were measured according to previous reports [12]. Briefly, excessive docetaxel and curcumin were added into various oils, surfactants, and co-surfactants and then the mixtures were shaken at 100 rpm under 37 °C for 72 h. Thereafter, the undissolved drug was separated by centrifugation at 12,000 rpm for 15 minutes. The contents of docetaxel and curcumin were determined by HPLC.

Construction of Pseudo-Ternary Phase Diagram (PTPD) and Preparation of DC- self-microemulsions (DC-SMEs)

In order to optimize microemulsion region (MA), pseudo-ternary phase diagram was constructed by mixing water, oil, surfactant and cosurfactant [23]. In brief, MCT was employed as the oil phase, DGME and EL40 were selected as surfactant and co-surfactant. The weight ratio of oil to surfactant were from 9:1 to 5:5. And the weight ratio of surfactant to co-surfactant were from 9:1 to 1:9. The mixtures was titrated dropwise into deionized water at 37°C with stirring of 300 r/min, and the phase behavior of the pseudo-ternary system (clarity and flowability) was monitored. When the mixture becomes cloudy and phase separation was observed, the titration end point is set. Based on these results, the MA was labelled in the ternary phase diagram using OriginPro 2019C 64-bit software.

Based on PTPD results, simplex lattice method analysis was used to optimize the ratio of oil phase, surfactant and co-surfactant. The percentage of oil phase (X_1), surfactant (X_2) and co-surfactant (X_3) were set as independent variables. The particle size (Y_1 ; nm) and drug (docetaxel and curcumin) loading efficiency (Y_2, Y_3 ; mg/g) were set as response variables. The percentage of independent variables of X_1 was in the range of 10% -25%, X_2 was in the range of 45% -60%, and X_3 was in the range of 30%-45%. The results were analyzed by using the software Design-Expert 8.0.6. The fitted polynomial equations were drawn in 3D response surfaces.

Characterization of DC-SMEs

Particle size, zeta potential and morphology of DC-SMEs

After diluted 100 times with distilled water, the particle size and zeta potential of DC-SMEs were measured by a dynamic light scattering (DLS) particle size analyzer (NanoZSE, Malvern Instruments Ltd., UK). The morphology of the DC-SMEs formulation was observed by a transmission electron microscope (TEM, Tecnai 12, Philips, Holland).

Stability of DC-SMEs

In order to evaluate the validity period of DC-SMEs, stability experiments was carried out. The DC-SMEs were stored at 4 °C for 30 days. After dilution with water, the droplet size and polydispersity index (PDI) of DC-SMEs were measured on day 0, day 5, day 10, day 15 and day 30.

In Vitro Drug Release of DC-SMEs

In vitro release of DC-SMEs was determined by the dialysis method. In brief, free docetaxel and curcumin and DC-SMEs were injected into dialysis bags (8000 ~ 14000 Da) and placed in a 250 ml pH 6.8 phosphate buffer containing 20% DMSO. Then, a series of samples were collected at 0.5, 1, 2, 4, 8 and 12 hours. The concentration of docetaxel and curcumin were analyzed by the HPLC method. All the experiments were carried out in triplicate.

Cytotoxicity Study of DC-SMEs

The cytotoxicity of DC-SMEs in Caco-2 cells in vitro was determined by MTT assay kit. Briefly, cells were seeded in 96-well plates with 1×10^5 cells per well in 200 μ l of complete medium. After 72 h exposure to the DC-SMEs at 37°C, cell viability was determined by MTT assay. All experiments were carried out in triplicate.

Caco-2 Cell Permeability of DC-SMEs and the Contribution of P-gp Protein

The permeability of DC-SMEs was evaluated by the transcellular transport experiment using Caco-2 monolayer. Briefly, Caco-2 cells were seeded on a 12-well transwell insert at the density of 1.0×10^5 cells/well for 21 days. Transepithelial resistance (TEER) increased by more than 250 was used for the permeability experiment. The permeability was determined on both the apical side and basolateral side. After incubation with the drug solutions (docetaxel and curcumin) or D-SMEs and DC-SMEs for 30 minutes, the samples were collected at 37°C at 15, 30, 45, 60, 90 and 120 minutes from the the apical side or basolateral side of the plate. All the experiments were conducted in triplicate. The concentration of docetaxel was measured by the UPLC-MS/MS method, and the apparent permeability coefficient (P_{app}) was calculated by the following formula:

$$P_{app} = dCr/dt \times V_r \times 1/A \times 1/C_0$$

where dCr/dt is the steady-state permeability rate (cm/s), V_r is the receiver volume, A is the diffusion area of the monolayer (cm²), and C_0 is the initial concentration of docetaxel. The concentrations were determined by the UPLC-MS/MS method.

In order to evaluate the role of P-gp protein in permeability, competitive inhibition experiment was performed. Briefly, caco-2 cells monolayer were incubated with DC-SMEs or a mixture of curcumin and docetaxel at 37°C for 45 minutes. And sterile PBS with or without verapamil as a control. After washing with cold PBS, the Caco-2 cells were homogenized with water. The samples were collected and centrifuged at 13000 rpm for 10 minutes, and the supernatant was analyzed by UPLC-MS/MS, and P_{app} was calculated by the formula.

In Vivo Pharmacokinetic Studies of DC-SMEs

The experimental plan was in line with institutional guidelines and approved by the Animal Health and Use Committee of Guang Xi University of Chinese Medicine.

Wister rats were randomly divided into two groups ($n = 4$), and were given free docetaxel or DC-SME orally (with a docetaxel equivalent dose of 20 mg/kg), respectively. Aliquots of blood samples were collected at 0.5, 1, 2, 3, 4, 6, 8, 12 and 24 hours, then transferred to heparinized tubes (10 mg/ml) and centrifuged at 12000 r for 3min. In order to calculate the absolute bioavailability, a physical mixture of curcumin and docetaxel was administered to rats by intravenous injection at a dose of 2mg/k. Aliquots of blood

samples were collected at 2, 5, 10, 20, 30 min and 1, 2, 4, 8, 12, and 24 hours. The supernatant was kept at -20 °C until it was analyzed. The absolute bioavailability was calculated by the following equation:

$$F = \text{AUC}_{\text{po}} \times D_{\text{iv}} / \text{AUC}_{\text{iv}} / D_{\text{po}} \times 100\%$$

where F refers to the absolute bioavailability, AUC_{po} refers to the area of oral, D_{iv} refers to the dose of intravenous, AUC_{iv} refers to the area of intravenous, and D_{po} refers to the dose of oral.

Statistical Analysis

Statistical analysis was conducted using the Bonferroni t-test after ANOVA for groups comparison and Student t test for two groups comparison at the $p < 0.05$ level. Results are expressed as mean \pm standard deviation (SD) from at least three individual samples.

Results And Discussion

Construction of Pseudo-Ternary Phase Diagram (PTPD) and Preparation of DC- self-microemulsions (DC-SMEs)

SMEs is a clear and isotropic system composed of oil, surfactant, and co-surfactant.

When exposed to the water environment of gastrointestinal tract (GI), ternary phase of SMEs spontaneously emulsified, forming oil-in-water nanoemulsion with droplet size of 10–250 nm. Therefore, it is very important to detect the solubility of drugs in three phases. Based on the results of solubility, we found that MCT, cremophor EL40, tween 80, tween 20, DGME and PEG 400 were the most effective in developing SMES because of their high solubility of docetaxel and curcumin (Table S1).

Surfactant and co-surfactants can be freely distributed between the oil and water phase as a modifier to reduce the interfacial tension and increase the stability of the emulsion, which are beneficial to the formation of the SMEs. In order to select appropriate co-emulsifiers and emulsifiers, a PTPD was plotted in the absence of curcumin and docetaxel. When MCT was used as the oil phase, the PTPDs of the different co-emulsifiers and emulsifiers were shown in Fig. 1a-f. Comparing the microemulsion area of three groups datas, it was found that the microemulsion area with PEG400 as co-emulsifier was larger than that with DGME as co-emulsifier, so PEG400 was selected as co-emulsifier. It is well known that the hydrophilic lipophilic balance (HLB) value is an important index for the selection of surfactants. The high HLB value indicates that the emulsifying ability of the emulsifier is strong. Although cremophor EL40, tween 80 and tween 20 could form O/W microemulsions with the same co-emulsifier (PEG400 or DGME), there was quite a difference in their emulsification ability. As shown in Fig. 1, cremophor EL 40 exhibited a higher microemulsion area than tween 80 and tween 20, so it was selected as emulsifier. And the HLB of tween 20 (HLB16.7) was higher than cremophor EL40 (HLB15) and tween 80 (HLB15) [24]. These results indicated the emulsification ability of surfactant is closely related to HLB and solubility. In the case of high drug solubility, the larger HLB of surfacant is beneficial for the SMEs.

Based on the results of PTPD, simplex lattice method analysis (SLMA) was used to optimize the ratio of oil phase, co-emulsifiers and emulsifiers. Design-Expert 8.0.6 software was used to analyze the interaction between the independent variables and response variables. 3D response surfaces were plotted in the Fig. 2. The polynomial regression equation was calculated as follows:

Particle size:

$$Y_1 = 915.2X_1 - 45.4X_2 - 137.2X_3 - 1170.5X_1X_2 - 885.4X_1X_3 + 471.8X_2X_3 (R^2 = 0.9854)$$

drug loading of curcumin:

$$Y_2 = -459.8X_1 - 426.2X_2 - 621.0X_3 + 1564.0X_1X_2 + 736.5X_1X_3 + 2189.1X_2X_3 (R^2 = 0.8857)$$

drug loading of docetaxel:

$$Y_3 = -685.2X_1 - 611.5X_2 - 898.8X_3 + 2291.1X_1X_2 + 1119.1X_1X_3 + 3173.7X_2X_3 (R^2 = 0.8913)$$

The p values are lower than 0.05, and the model fits well.

According to the optimization result, the optimal percentage of oil for DC-SMEs was 10.0% (w/w) and the emulsifiers and co-emulsifiers were 52.5% (w/w) and 37.5% (w/w), respectively. As shown in Table S2, there is no significant difference between the predicated and measured value of particle size and loading efficiency (the deviation was less than 2%), which indicated that the obtained fitting equation could accurately describe the relationship between the independent variables and response variables.¹¹

Figure 2 showed that with the increase of cremophor EL 40 and PEG400, particle size decreases. By contrast, the drug loading of curcumin and docetaxel gradually increased with the increase of cremophor EL 40 and PEG 400, and then decreased slightly.

Characterization of DC-SMEs

After diluted 100 times with deionized water, the droplet size, zeta potential and TEM image of DC-SMEs were measured and the results were shown in Fig. 3. It was observed that SMEs quickly dispersed in water within 20 s, and the appearance of micro-emulsion was light yellow. The DLS results showed that the droplet size and zeta potential of DC-SMEs were 32.23 ± 2.21 nm and 16.25 ± 3.72 mv, respectively. These results indicated that prepared SMEs had an excellent self-nanoemulsifying ability. TEM images clearly showed that many spherical micro-emulsion droplets are formed after hydration, and they are spherical with a diameter of 30 nm, which was in good agreement with DLS. Generally speaking, the

droplet size of SMEs smaller than 300 nm is considered to be more suitable for endocytosis [25]. Thus, the optimal particle size of 30 nm will show excellent intestinal permeability and oral bioavailability. In addition, the stability results showed that after 30 days storage at 4°C, there was no obvious change in the appearance, particle size and PDI, which indicated that DC-SMEs had good stability (Fig. 3).

In vitro release experiment of DC-SMEs was performed in pH 6.8 phosphate buffer containing 20% DMSO, which was the sink condition of docetaxel. After 12 hours inculcured in pH 6.8 buffer, the cumulative release rates of docetaxel and curcumin were $69.2 \pm 8.9\%$ and $78.0 \pm 3.1\%$ after 12 h, respectively (Fig. 4). The steady release behavior indicated that there is a strong interaction between drugs and SMEs, which may provide protection for drugs in gastrointestinal tract. Compare to DC-SMEs, D-SMEs showed a similar release pattern of docetaxel, which indicated that co-loading curcumin did not interfere with docetaxel release. Notably, curcumin exhibited a higher release rate than that of docetaxel in DC-SMEs. The released curcumin may inhibit p-gp, which was beneficial to the absorption of the released docetaxel, thus improving oral bioavailability. Therefore, co-encapsulation of docetaxel and curcumin in SMEs was a potential platform for promoting drug dissolution, release and absorption.

Cytotoxicity Study of DC-SMEs

In order to evaluate the cytotoxicity of DC-SMEs, Caco-2 cells were used to carry out MTT assay. As shown in Fig. 5, no obvious cytotoxicity was observed in the presence of docetaxel, curcumin and DC-SMEs ranging from 1–10 μM , which was used in the following permeability evaluation.

Caco-2 Cell Permeability of DC-SMEs and the Contribution of P-gp Protein

The membrane permeability was determined by calculating P_{app} using Caco-2 mono-layer, and the results were shown in Fig. 6 In the free docetaxel group, the P_{app} was $(0.3 \pm 0.05) \times 10^{-6}$ cm/s, which suggested a poor permeability of docetaxel. By contrast, loading docetaxel in D-SMEs increased the permeability of docetaxel by 1.8 times, which indicated the larger surface area of nanoparticles promoting drug release and transmembrane. Although D-SMEs exhibited better permeability than free docetaxel, the P_{app} of D-SMEs was significantly higher in the B-A direction than in the A-B direction ($(1.1 \pm 0.08) \times 10^{-6}$ cm/s vs $(2.4 \pm 0.13) \times 10^{-6}$ cm/s) [26]. These results indicated that D-SMEs can not overcome the efflux effect of the P-gp. In order to reduce the inhibitory effect of P-gp, a typical inhibitor verapami [27] (or curcumin¹⁸) was co-incubated with docetaxel. The results suggested the P_{app} of docetaxel was increased by 4.6 and 3.8 times in the presence of verapami and curcumin. By contrast, DC-SMEs showed a similar P_{app} , which indicated that the improvement permeability of DC-SMEs was due to the inhibition of P-gp by curcumin. Therefore, loading p-gp inhibitor in SMEs is an effective strategy to overcome drug resistance.

In Vivo Pharmacokinetic (PK) Studies of DC-SMEs

A comparative pharmacokinetic study was conducted to evaluate the oral absorption of free drugs and SMEs. After the oral dose of 20 mg/kg, the plasma concentration-time curves and the pharmacokinetic

parameters of docetaxel, D-SMEs and DC-SMEs were compared. As shown in Fig. 7, D-SMEs prolonged the in vivo half-life of the free docetaxel by 3.7 fold compare with free docetaxel, indicating the sustained release of SMEs. Compared with free docetaxel, the AUC_{0-24h} of D-SMEs was increased by 3.1 times, which suggested the SMEs could improve improve the solubility and release of docetaxel, and thus improve its oral bioavailability. However, the efflux effect of P-gp significantly decreased the oral absorption of D-SMEs.

In contrast, the parameters AUC_{0-24} and C_{max} of DC-SMEs were increased by 1.6 times and 1.5 times compared to D-SMEs, respectively (Table S2). The absolute bioavailabilities of docetaxel increasing from 0.9% in free drug to 2.9% in D-SMEs and 4.8% in DC-SMEs. These results suggested DC-SMEs was a potent platform to improve the oral bilavailability of docetaxle. In addition, the AUC_{0-24} of curcumin was $784.7 \pm 61.0 \mu\text{g}\cdot\text{h}\cdot\text{L}^{-1}$, which indicated that its excellent release from DC-SMEs in vivo. Combined with the results of in vitro release experiment, the cumulative release of curcumin in pH 6.8 buffer was more than 70%, and its release rate was superior than that of docetaxel. Therefore, we proved that co-delivery of curcumin could inhibit the p-gp protein, and thus improving the oral bioavailability of docetaxel.

Oral chemotherapy with docetaxel is also restricted by its hepatic first-pass metabolism. As shown in Table 1, the $t_{1/2}$ of DC-SMEs was 1.7 times higher than that of D-SMEs, which indicated the co-loading of curcumin could limit CYP metabolism of docetaxel [21]. Importantly, co-loaded DC-SMEs showed a long-term high plasma concentration of more than 120 ng/ml for about 25 h (Fig. 7). The results indicated that high oral bioavailability of DC-SMEs was related to the inhibitory effect of CYP 450.

Table 1

Pharmacokinetic parameters of docetaxel in plasma after oral administration of D-SMEs and DC-SMEs at a dose of 20 mg/kg and I.V. administration of docetaxel at a dose of 2 mg/kg, respectively.

PK parameters	$AUC_{0-24h} / (\mu\text{g}\cdot\text{h}\cdot\text{L}^{-1})$	$t_{1/2}/\text{h}$	$C_{max} / (\mu\text{g}\cdot\text{L}^{-1})$	t_{max}/h
Docetaxel (i.v.)	4048.2 ± 2812.8	6.3 ± 4.9	1657.8 ± 1495.2	0.083
DC-SMES-curcumin (p.o.)	784.7 ± 61.0	7.7 ± 4.1	266.2 ± 91.9	3 ± 0.7
docetaxel (p.o.)	384.5 ± 116.7	3.8 ± 3.0	135.8 ± 13.1	4 ± 0.8
D-SMES-docetaxel (p.o.)	1180.4 ± 197.4	$13.9 \pm 8.4^*$	$401.7 \pm 30.4^*$	3 ± 0.4
DC-SMES-docetaxel (p.o.)	$1946.5 \pm 102.6^*$	$23.0 \pm 1.9^*$	$621.3 \pm 120.9^*$	3 ± 0.6

AUC_{0-t} : area under the plasma concentration-time profiles from time 0 to the last time point. $t_{1/2}$: elimination half-life. C_{max} : peak plasma concentration. T_{max} : time to reach peak plasma concentration. * $p < 0.01$ compared with free docetaxel group.

Conclusion

In summary, docetaxel and curcumin were successfully co-encapsulated into SMEs with a rapid self-nanoemulsifying rate. Optimized SMEs with a size of 30 nm showed excellent stability within 30 days and steady sequential release behavior. More importantly, the DC-SMEs significantly improved the solubility, permeability and oral bioavailability of docetaxel by simultaneously limiting the efflux of P-gp and the first-pass metabolism of liver. Therefore, DC-SMEs exhibited great potential in novel oral docetaxel development.

Declarations

Acknowledgment This work was financially supported by the National Nature Science Foundation of China (No. 82060641), and China postdoctoral fund (2019M653814XB).

Author contribution These authors contributed equally to this work.

Data availability The data that support the findings of this study are available on request from the corresponding author.

Ethics approval and consent to participate All the animal procedures were performed in accordance with the guidelines for the care and use of laboratory animals.

Consent for publication All authors have approved that the submitted works are original, and the work has not been published and is not being considered for publication elsewhere.

Competing interests The authors declared no competing interests.

References

1. Koolen SL, Beijnen JH, Schellens JH. Intravenous-to-oral switch in anticancer chemotherapy: a focus on docetaxel and paclitaxel. *Clin Pharmacol Ther.* 2010;87(1):126–9. <https://doi.org/10.1038/clpt.2009.233>.
2. Tannock IF, de Wit R, Berry WR, Horti J, Pluzanska A, Chi KN, Oudard S, Théodore C, James ND, Turesson I, Rosenthal MA, Eisenberger MA. TAX 327 Investigators. Docetaxel plus prednisone or mitoxantrone plus prednisone for advanced prostate cancer. *N Engl J Med.* 2004;351(15):1502–12. <https://doi.org/10.1056/NEJMoa040720>.
3. Vermunt MAC, Robbrecht DGJ, Devriese LA, Janssen JM, Thijssen B, Keessen M, van Eijk M, Kessels R, Eskens FALM, Beijnen JH, Mehra N, Bergman AM. ModraDoc006, an oral docetaxel formulation in combination with ritonavir (ModraDoc006/r), in metastatic castration-resistant prostate cancer patients: A phase Ib study. *Cancer Rep (Hoboken).* 2021;4(4):e1367. <https://doi.org/10.1002/cnr2.1367>.
4. Engels FK, Verweij J. Docetaxel administration schedule: from fever to tears? A review of randomised studies. *Eur J Cancer.* 2005;41(8):1117–26. <https://doi.org/10.1016/j.ejca.2005.02.016>.

5. Jibodh RA, Lagas JS, Nuijen B, Beijnen JH, Schellens JH. Taxanes: old drugs, new oral formulations. *Eur J Pharmacol.* 2013;717(1–3):40–6. <https://doi.org/10.1016/j.ejphar.2013.02.058>.
6. Sawicki E, Beijnen JH, Schellens JHM, Nuijen B. Pharmaceutical development of an oral tablet formulation containing a spray dried amorphous solid dispersion of docetaxel or paclitaxel. *Int J Pharm.* 2016;511(2):765–73. <https://doi.org/10.1016/j.ijpharm.2016.07.068>.
7. Valicherla GR, Dave KM, Syed AA, Riyazuddin M, Gupta AP, Singh A, Wahajuddin, Mitra K, Datta D, Gayen JR. Formulation optimization of Docetaxel loaded self-emulsifying drug delivery system to enhance bioavailability and anti-tumor activity. *Sci Rep.* 2016;6:26895. <https://doi.org/10.1038/srep26895>.
8. Feng QP, Zhu YT, Yuan YZ, Li WJ, Yu HH, Hu MY, Xiang SY, Yu SQ. Oral administration co-delivery nanoparticles of docetaxel and bevacizumab for improving intestinal absorption and enhancing anticancer activity. *Mater Sci Eng C Mater Biol Appl.* 2021;124:112039. <https://doi.org/10.1016/j.msec.2021.112039>.
9. Sun B, Luo C, Li L, Wang M, Du Y, Di D, Zhang D, Ren G, Pan X, Fu Q, Sun J, He Z. Core-matched encapsulation of an oleate prodrug into nanostructured lipid carriers with high drug loading capability to facilitate the oral delivery of docetaxel. *Colloids Surf B Biointerfaces.* 2016;143:47–55. <https://doi.org/10.1016/j.colsurfb.2016.02.065>.
10. Soulele K, Karampelas T, Tamvakopoulos C, Macheras P. Enhancement of Docetaxel Absorption Using Ritonavir in an Oral Milk-Based Formulation. *Pharm Res.* 2021;38(8):1419–28. <https://doi.org/10.1007/s11095-021-03085-x>.
11. Wang Y, Huang J, Wang Z, Wang X, Liu H, Li X, Qiao H, Wang L, Chen J, Chen X, Li J. Extra virgin olive oil-based phospholipid complex/self-microemulsion enhances oral absorption of salvianolic acid B through inhibition of catechol-O-methyltransferase-mediated metabolism. *Int J Pharm.* 2022;611:121330. <https://doi.org/10.1016/j.ijpharm.2021.121330>.
12. Liu H, Mei J, Xu Y, Tang L, Chen D, Zhu Y, Huang S, Webster TJ, Ding H. Improving The Oral Absorption Of Nintedanib By A Self-Microemulsion Drug Delivery System: Preparation And In Vitro/In Vivo Evaluation. *Int J Nanomedicine.* 2019;14:8739–51. <https://doi.org/10.2147/IJN.S224044>.
13. Hendriks JJMA, Stuurman FE, Song JY, de Weger VA, Lagas JS, Rosing H, Beijnen JH, Schinkel AH, Schellens JHM, Marchetti S. No relation between docetaxel administration route and high-grade diarrhea incidence. *Pharmacol Res Perspect.* 2020;8(4):e00633. <https://doi.org/10.1002/prp2.633>.
14. Cui W, Zhao H, Wang C, Chen Y, Luo C, Zhang S, Sun B, He Z. Co-encapsulation of docetaxel and cyclosporin A into SNEDDS to promote oral cancer chemotherapy. *Drug Deliv.* 2019;26(1):542–50. <https://doi.org/10.1080/10717544.2019.1616237>.
15. Jalaeikhoo H, Khajeh-Mehrzi A. Immunosuppressive therapy in patients with aplastic anemia: a single-center retrospective study. *PLoS One.* 2015;10(5):e0126925. <https://doi.org/10.1371/journal.pone.0126925>.
16. Murray BM, Paller MS, Ferris TF. Effect of cyclosporine administration on renal hemodynamics in conscious rats. *Kidney Int.* 1985;28(5):767–74. <https://doi.org/10.1038/ki.1985.196>.

17. Wu SH, Hang LW, Yang JS, Chen HY, Lin HY, Chiang JH, Lu CC, Yang JL, Lai TY, Ko YC, Chung JG. Curcumin induces apoptosis in human non-small cell lung cancer NCI-H460 cells through ER stress and caspase cascade- and mitochondria-dependent pathways. *Anticancer Res.* 2010;30(6):2125–33. <https://doi.org/10.1097/CAD.0b013e328338b6a5>.
18. Chao S, Lv X, Ma N, Shen Z, Zhang F, Pei Y, Pei Z. A supramolecular nanoprodruge based on a boronate ester linked curcumin complexing with water-soluble pillar[5]arene for synergistic chemotherapies. *Chem Commun (Camb).* 2020;56(62):8861–4. <https://doi.org/10.1039/D0CC04315J>.
19. Hou S, Zhou S, Chen S, Lu Q. Polyphosphazene-Based Drug Self-Framed Delivery System as a Universal Intelligent Platform for Combination Therapy against Multidrug-Resistant Tumors. *ACS Appl Bio Mater.* 2020;3(4):2284–94. <https://doi.org/10.1021/acsabm.0c00072>.
20. Rejinold NS, Yoo J, Jon S, Kim YC. Curcumin as a Novel Nanocarrier System for Doxorubicin Delivery to MDR Cancer Cells: In Vitro and In Vivo Evaluation. *ACS Appl Mater Interfaces.* 2018;10(34):28458–28470. <https://doi.org/10.1021/acsami.8b10426>.
21. Shamsi S, Tran H, Tan RS, Tan ZJ, Lim LY. Curcumin, Piperine, and Capsaicin: A Comparative Study of Spice-Mediated Inhibition of Human Cytochrome P450 Isozyme Activities. *Drug Metab Dispos.* 2017;45(1):49–55. <https://doi.org/10.1124/dmd.116.073213>.
22. Cheng AL, Hsu CH, Lin JK, Hsu MM, Ho YF, Shen TS, Ko JY, Lin JT, Lin BR, Ming-Shiang W, Yu HS, Jee SH, Chen GS, Chen TM, Chen CA, Lai MK, Pu YS, Pan MH, Wang YJ, Tsai CC, Hsieh CY. Phase I clinical trial of curcumin, a chemopreventive agent, in patients with high-risk or pre-malignant lesions. *Anticancer Res.* 2001;21(4B):2895–900. <https://doi.org/10.1110/ps.0212902>.
23. Sawatdee S, Atipairin A, Sae Yoon A, Srichana T, Changsan N, Suwandecha T. Formulation Development of Albendazole-Loaded Self-Microemulsifying Chewable Tablets to Enhance Dissolution and Bioavailability. *Pharmaceutics.* 2019;11(3):134. <https://doi.org/10.3390/pharmaceutics11030134>.
24. Foo KS, Bavoh CB, Lal B, Mohd Shariff A. Rheology Impact of Various Hydrophilic-Hydrophobic Balance (HLB) Index Non-Ionic Surfactants on Cyclopentane Hydrates. *Molecules.* 2020;25(16):3725. <https://doi.org/10.3390/molecules25163725>.
25. Ahmad N, Alam MA, Ahmad R, Umar S, Jalees Ahmad F. Improvement of oral efficacy of Irinotecan through biodegradable polymeric nanoparticles through in vitro and in vivo investigations. *J Microencapsul.* 2018c;35:327–43. <https://doi.org/10.1080/02652048.2018.1485755>.
26. Yin YM, Cui FD, Mu CF, Choi MK, Kim JS, Chung SJ, Shim CK, Kim DD. Docetaxel microemulsion for enhanced oral bioavailability: preparation and in vitro and in vivo evaluation. *J Control Release.* 2009;140(2):86–94. <https://doi.org/10.1016/j.jconrel.2009.08.015>.
27. Wang L, Sun Y. Efflux mechanism and pathway of verapamil pumping by human P-glycoprotein. *Arch Biochem Biophys.* 2020;696:108675. <https://doi.org/10.1016/j.abb.2020.108675>.

Figures

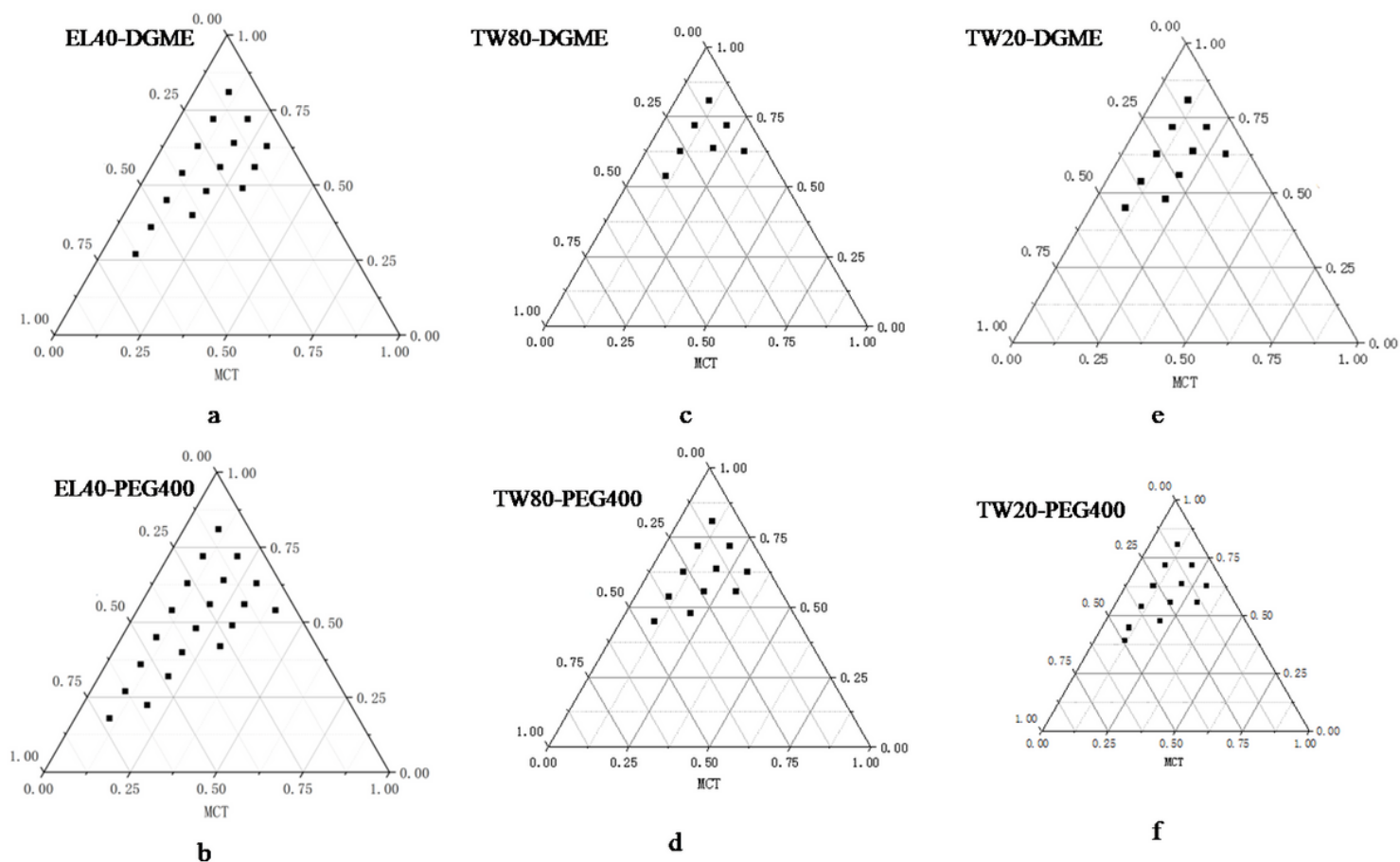


Figure 1

PTPD of various surfactant, co-surfactant, oil, and water. a: MCT/Cremophor EL40/DGME system; b: MCT/Cremophor EL40/PEG400 system; c: MCT/TW80/DGME system; d: MCT/TW80/PEG400 system; e: MCT/TW20/DGME system; f: MCT/TW20/PEG400 system. Microemulsion regions of the ternary plot are expressed in dot.

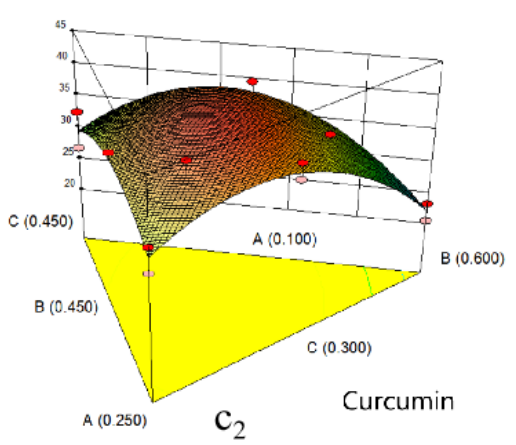
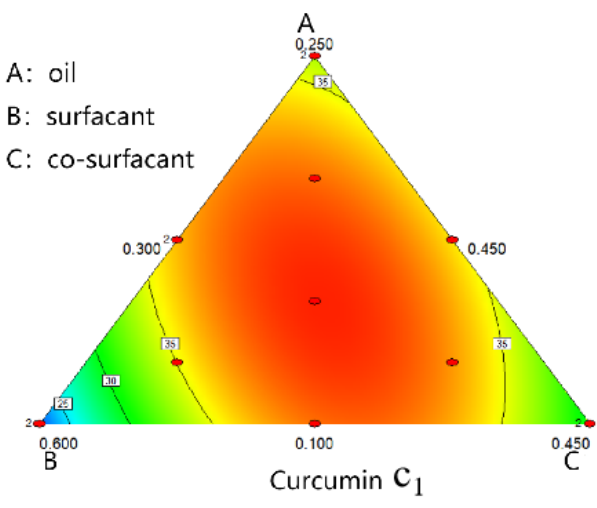
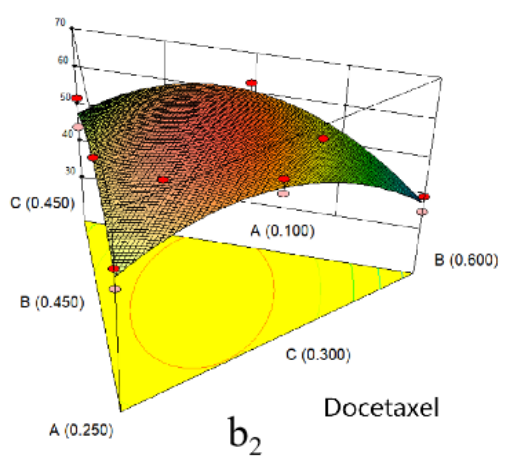
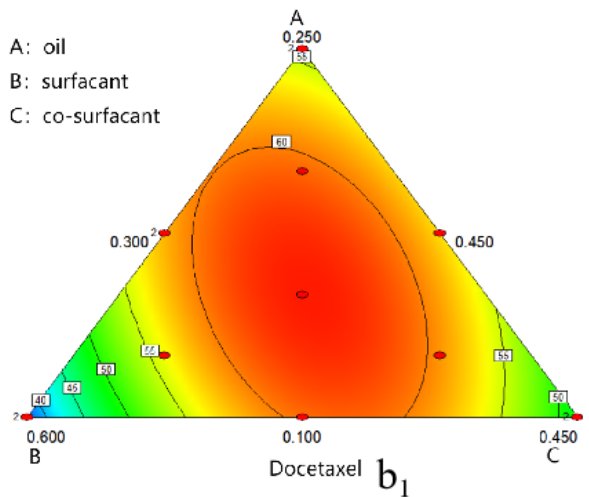
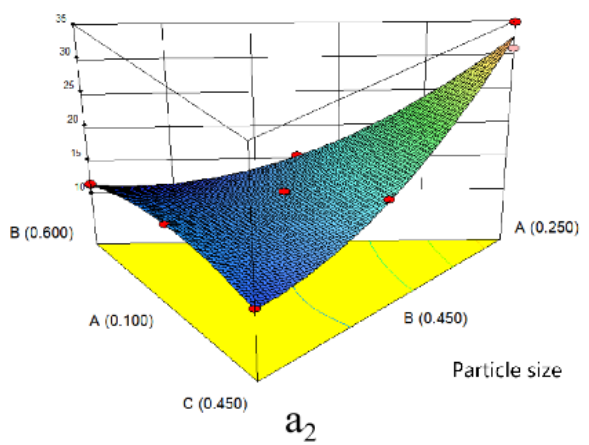
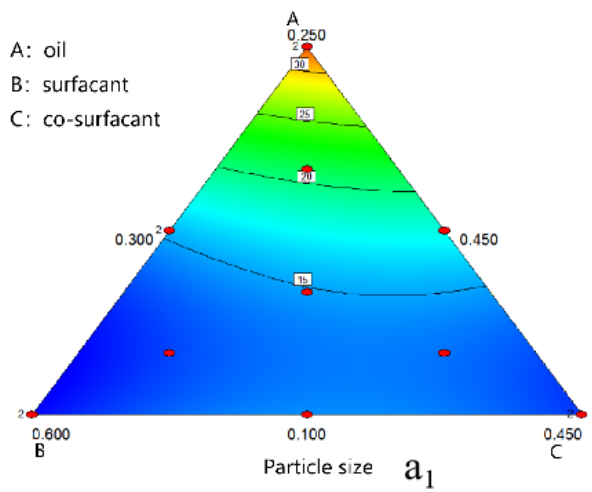


Figure 2

Three-dimensional response surface diagrams for the influence of the ratio of oil phase, surfactant and co-surfactant on droplet size (a), docetaxel loading (b) and curcumin loading(c).

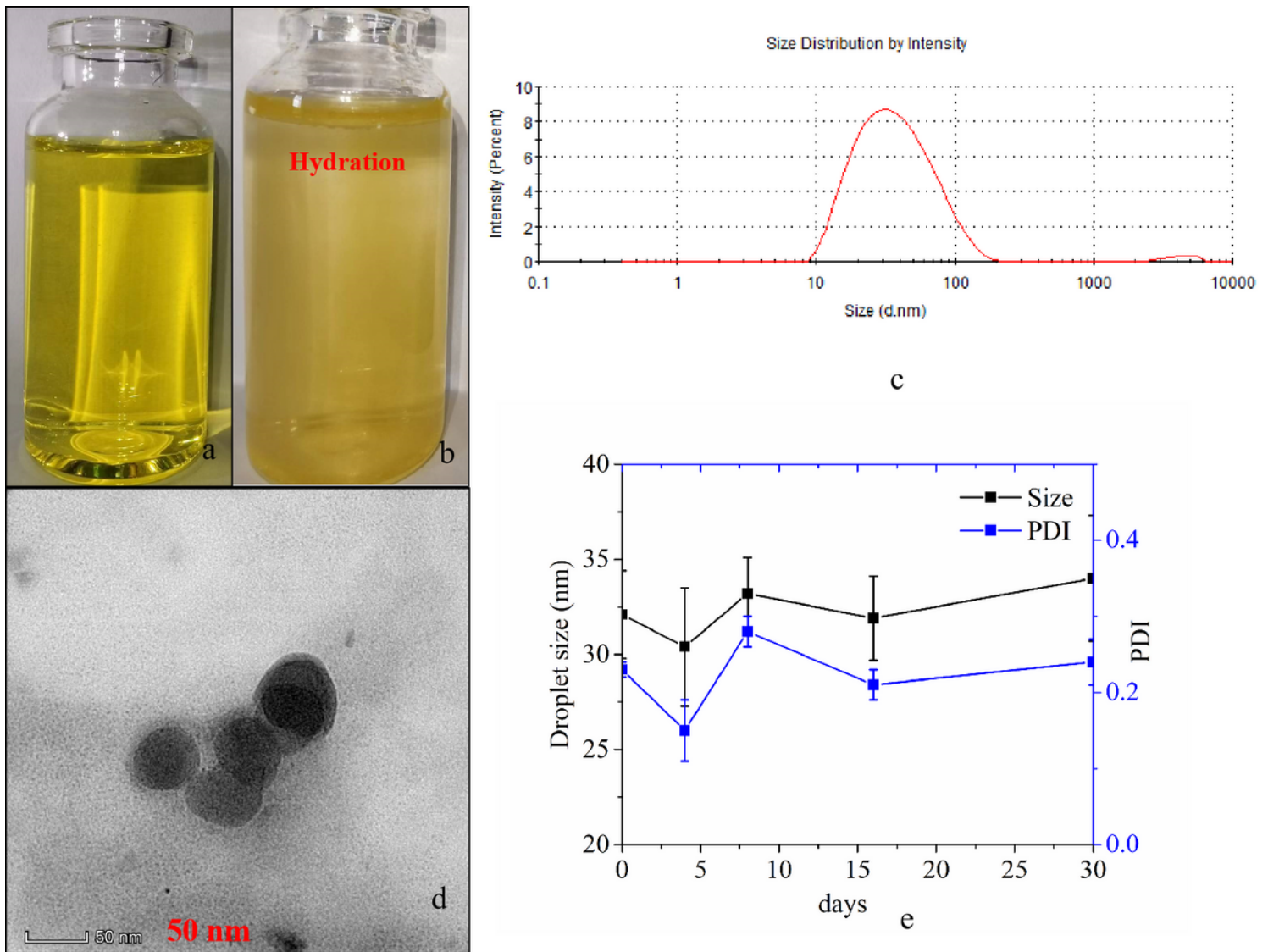


Figure 3

a, b: Appearance of DC-SMEs; c: droplet size distribution of DC-SMEs; d: morphology of DC-SMEs; e: the particle size and zeta potential of DC-SMEs storage at 4 °C for 30 days (n=3).

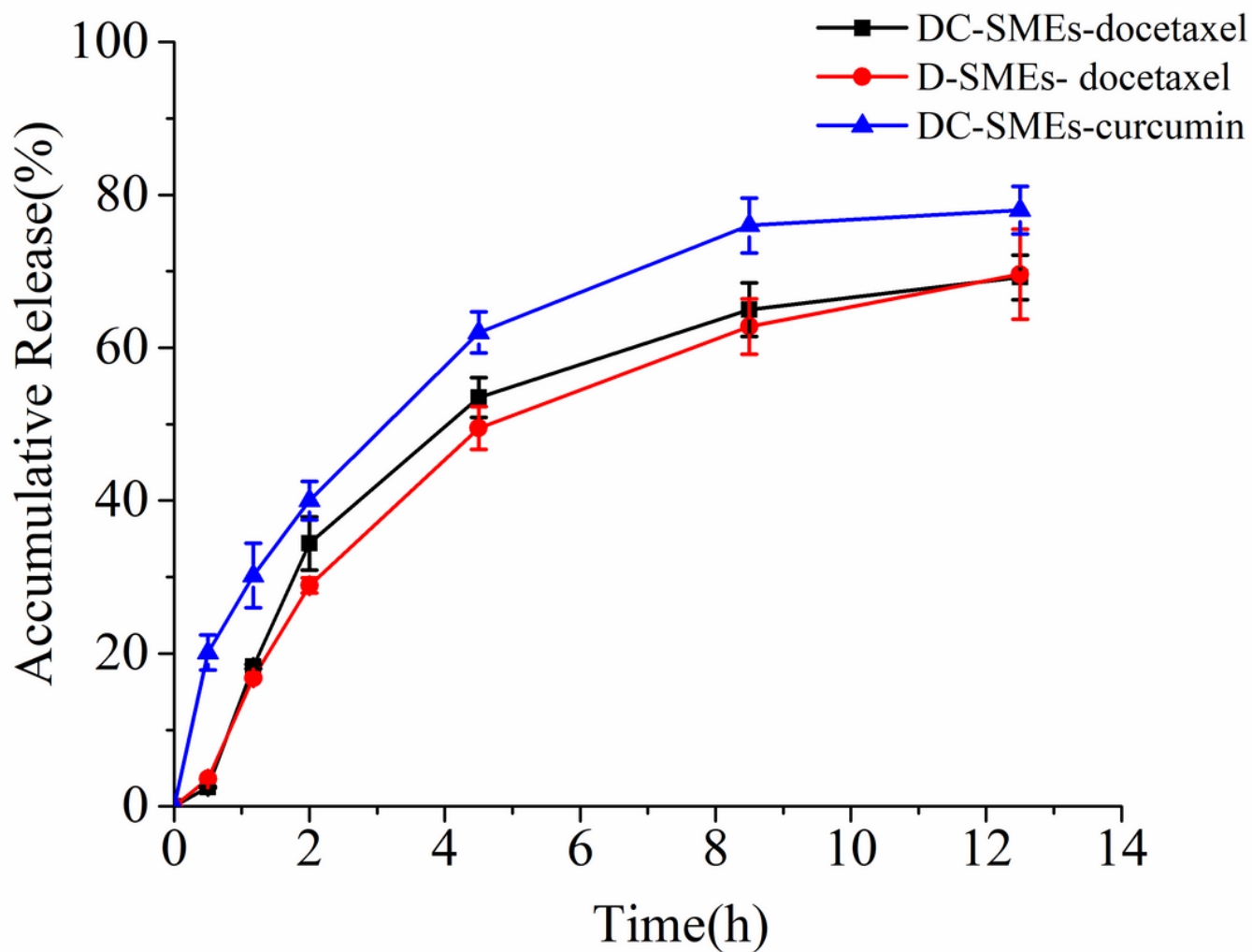


Figure 4

The cumulative release profile of DC-SMEs and D-SMEs in pH 6.8 phosphate buffer containing 20% DMSO (n=3).

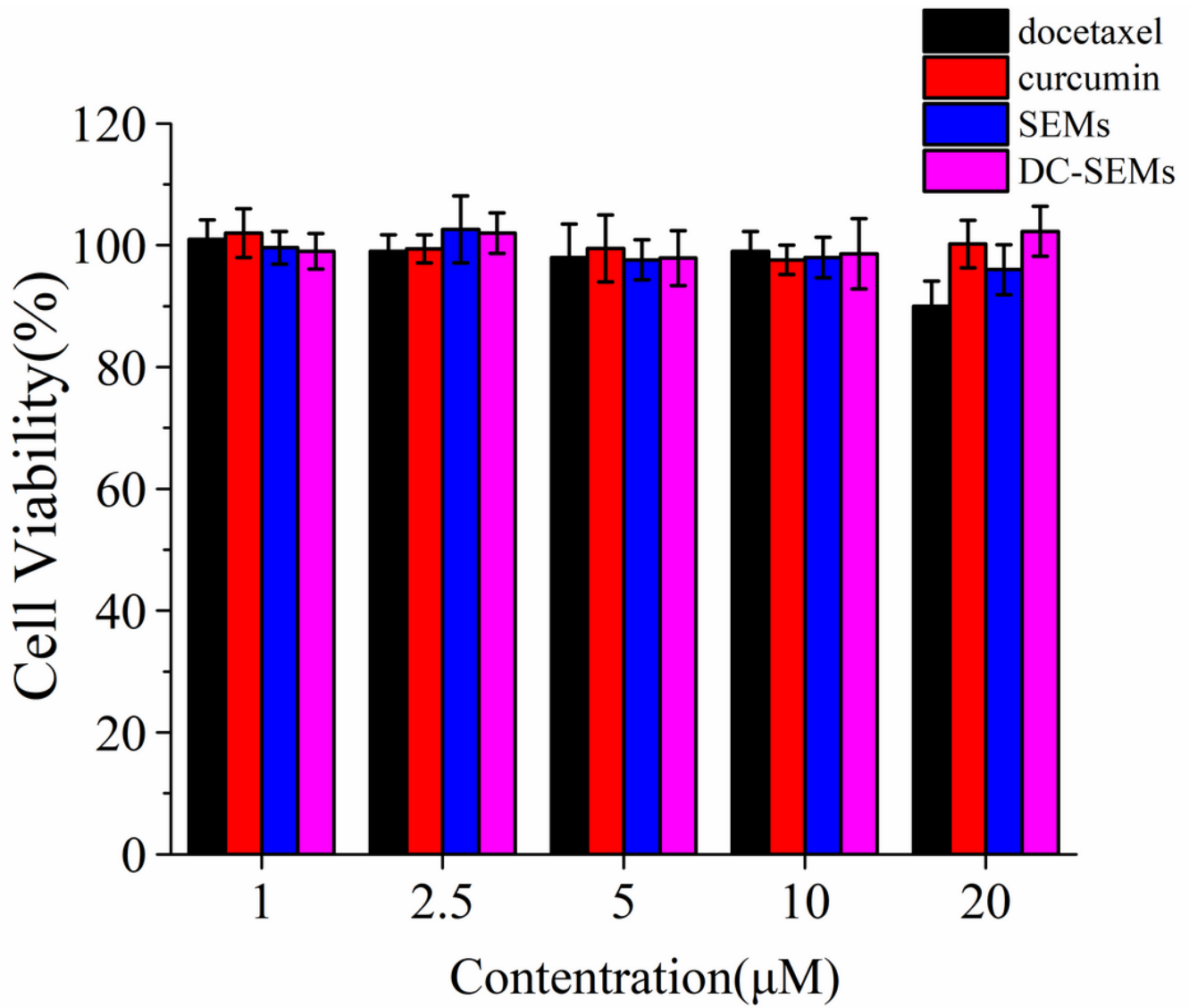


Figure 5

Relative viability of Caco-2 cells treated with free docetaxel, curcumin and DC-SMEs ranged from 1-20 μM for 72 h (n=6).

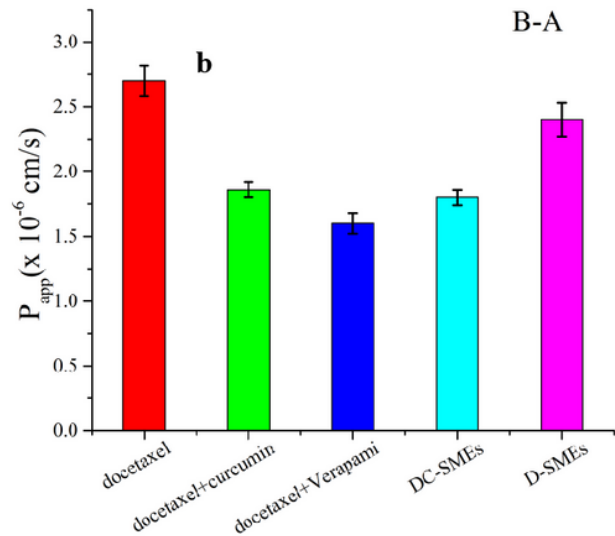
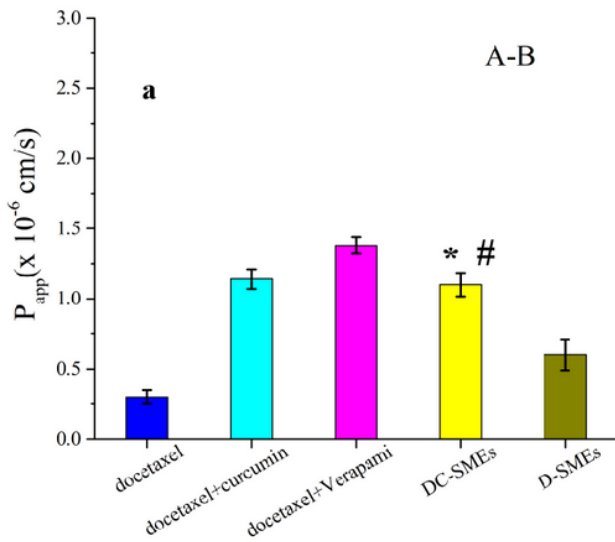


Figure 6

P_{app} of docetaxle for free docetaxel, mixture of docetaxel and curcumin, mixture of docetaxel and verapami, DC-SMEs and D-SMEs passed through the Caco-2 monolayer during the transportation from apical-to-basolateral (AP-BL) and basolateral-to-apical(n=6, *means compared to free docetaxel, # means compared with D-SMEs, *p < 0.01, #p < 0.01).

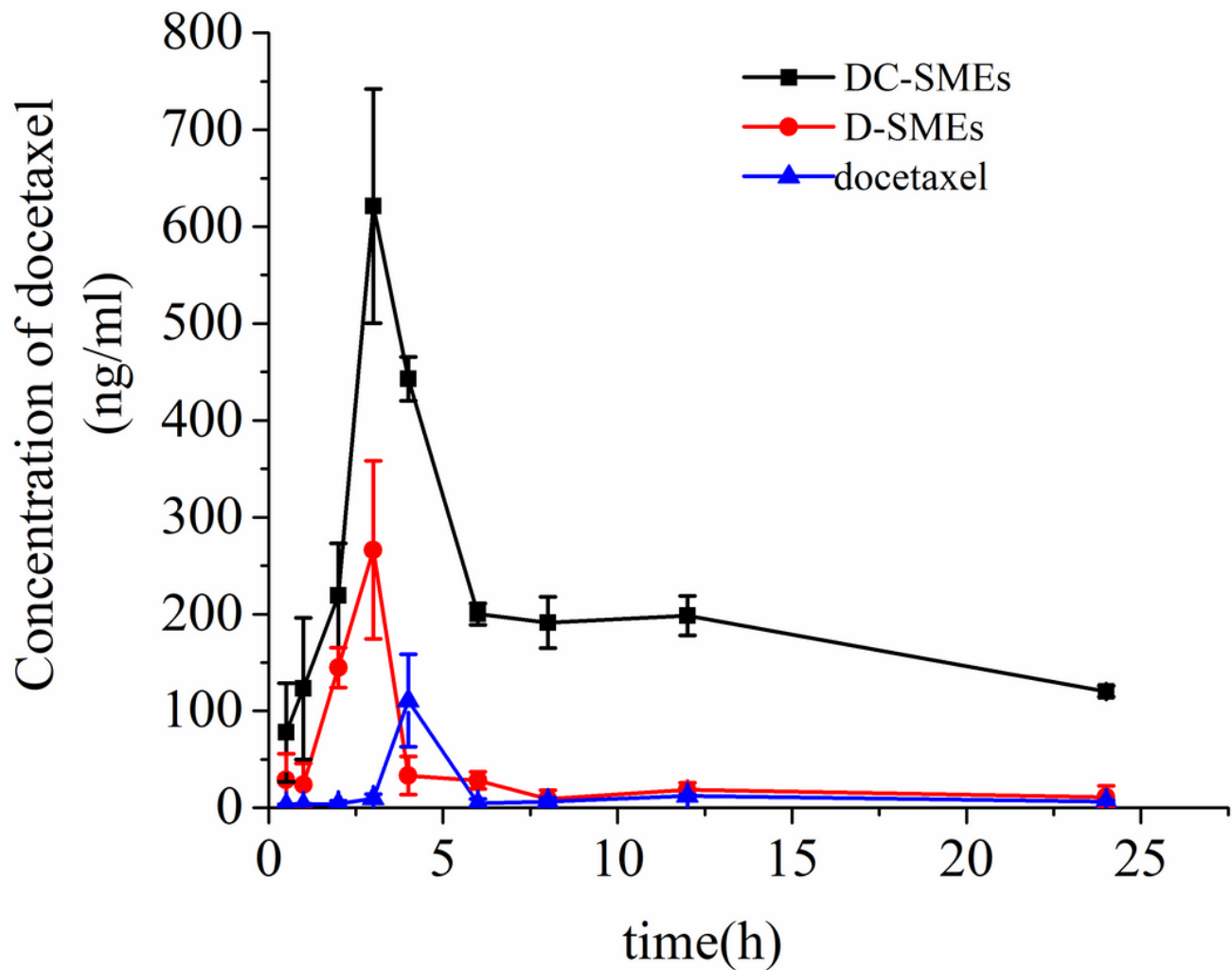


Figure 7

Plasma concentration-time profiles of docetaxel following a single oral administration of free docetaxel, D-SMEs and DC-SMEs at a dose of 20mg/kg (docetaxel equivalent, n=4).

Supplementary Files

This is a list of supplementary files associated with this preprint. Click to download.

- [GraphicalAbstract.docx](#)
- [SupplementaryMaterial.doc](#)